

CRYSTALLOGRAPHIC STUDIES OF THE BINDING OF LIGANDS TO THE DICARBOXYLATE SITE OF Complex II, AND THE IDENTITY OF THE LIGAND IN THE "OXALACETATE-INHIBITED" STATE.

Li-Shar Huang, John T. Shen, Andy C. Wang, Edward A. Berry.  
Physical Biosciences Division; Lawrence Berkeley National Lab., Berkeley CA 94720

**Abstract-**

Mitochondrial Complex II (succinate:ubiquinone oxidoreductase) is purified in a partially inactivated state, which can be activated by removal of tightly bound oxaloacetate (Kearney, E. B. et al. *Biochem Biophys Res Commun* 49, 1115-1121). We crystallized Complex II in the presence of oxalacetate or with the endogenous inhibitor bound. The structure showed a ligand essentially identical to the "malate-like intermediate" found in *Shewanella* Flavocytochrome c crystallized with fumarate (Taylor, P. et al. *Nat Struct Biol* 6, 1108-1112.) Crystallization of complex II in the presence of excess fumarate gave variable results: in one case, fumarate was found in the site but under different conditions, the malate-like intermediate was found. In order to more conveniently monitor the occupation state of the dicarboxylate site, we are developing a library of UV/Vis spectral effects induced by binding different ligands to the site. Treatment with fumarate results in rapid development of the fumarate difference spectrum and then a very slow conversion into a species spectrally similar to the OAA-liganded complex. Complex II is known to be capable of oxidizing malate to the enol form of oxalacetate (Belikova, Y. O. et al. *Biochim Biophys Acta* 936, 1-9). The observations above suggest it may also be capable of interconverting fumarate and malate. It may be useful for understanding the mechanism and regulation of the enzyme to identify the malate-like intermediate and its pathway of interconversion with oxaloacetate and fumarate.

**Introduction-**

Complex II catalyzes one step of the Krebs tricarboxylic acid cycle, oxidation of succinate to fumarate. This step is unique, among the oxidative steps of the Krebs cycle, in coupling the oxidation to the ubiquinone pool rather than NAD/NADH, and the reason for this is clear if one examines the redox midpoint potentials of the Krebs cycle reactions. The succinate/fumarate couple has a midpoint potential around +25 mv at pH 7, much higher than that of the NADH/NAD<sup>+</sup> couple and thus incapable of reducing the latter under normal conditions or at a kinetically competent rate. The other three oxidations of the Krebs cycle have considerably more reducing power: the weakest being the malate/oxaloacetate couple ( $E_m^7 = -166$  mv). Thus the unique status of complex II, as the only member of the Krebs cycle that is membrane bound and part of the respiratory chain, can be seen as an adaptation to let this weakest step of the cycle avoid some work by bypassing Complex I and coupling site 1.

Early investigators of Complex II found that, in submitochondrial particles, purified complex II or soluble succinate dehydrogenase preparations, the enzyme was in a relatively inactivated state. Various seemingly unrelated treatments were developed to bring it to a higher, constant level of activity [1]. Later it was realized that all of these treatments resulted in removal of tightly bound oxaloacetate (OAA) in parallel with activation of the dehydrogenase [2]. Both activation and OAA removal show a high activation energy, proceeding at a negligible rate at 4°C and on a time scale of tens of minutes at room temperature.

OAA binds as a classical competitive inhibitor, with a dissociation constant that can be calculated from the ratio of on and off rate constants [3]. However due to the extremely low dissociation rate ( $\sim 0.02 \text{ min}^{-1}$  [3]) it does not equilibrate on the time-course of a normal enzyme assay, and appears more like an irreversible inhibitor on this time scale. The physiological significance of this inhibition by OAA is not clear (at least to the present authors), however it is to be noted that OAA is the end product of the Krebs cycle, and would be expected to accumulate under conditions where the supply of reduced two-carbon units to acetyl CoA from glycolysis or fatty acid metabolism is interrupted. The competitive nature of the inhibition allows high concentration of succinate to overcome the inhibition, however the relative affinity of the oxidized enzyme for succinate is  $\sim 600$  times lower than that for OAA [3].

It has been clearly shown. [4-6] that in addition to oxidizing succinate, Complex II also oxidizes **D-** or **L-** malate to (the enol form of) OAA. While this may not seem particularly surprising in light of the structural similarity between succinate and malate or fumarate and enol-OAA, it raises a number of interesting points.

First there is the question of an energetic leak: malate oxidation is normally coupled to the NADH pool by malate dehydrogenase. Not only would oxidation of malate by succinate bypass complex I and decrease the efficiency of energy conversion from this step, but simultaneous operation of both enzymes would result in a futile cycle in which malate would be oxidized by complex II and re-reduced by MDH, draining the NADH pool directly to the Q pool. This would eliminate the driving force for complex I, and reversed electron transport through Complex I would dissipate any protonmotive force that may be generated by other electron transfer complexes or the ATPase. Needless to

say this doesn't happen, at least in part because the rate of malate oxidation is quite feeble, about  $8 \text{ min}^{-1}$  at best with L-malate[6]. Still it might be expected that evolutionary pressure would stop this leak entirely, by regulation if not at the level of enzyme specificity, unless perhaps it plays some role as a safety valve to get the system out of some unusual redox state.

Another consequence of malate oxidation by complex II, together with the fact that the product OAA is an inhibitor with an extremely low off-rate, is that malate is a suicide inhibitor of complex II. The highly exergonic oxidation of malate by ubiquinone contributes to the driving force for loading the enzyme with OAA despite the low rate. Surprisingly, the Complex-II-catalyzed malate dehydrogenase reaction runs for several turnovers at a rate higher than the dissociation rate of tightly bound OAA. This suggests that the form of the enzyme with tightly-bound OAA is different from the initial product complex from malate oxidation[6]. This seems not to be a matter of tautomerization, as the enol form of OAA which is produced by malate oxidation is the form which most rapidly inhibits succinate oxidation[6].

Crystallographic studies of Complex II have lagged behind those of complexes III and IV. This may seem surprising in that the bottleneck in these studies is preparation of crystals, and it would be expected that Complex II, with a greater proportion of mass in the water-exposed subunits 1 and 2 relative to transmembrane region (subunits 3 and 4) would be relatively easy to crystallize. It may be that the monotopic nature of the protein, with hydrophilic surface on only one side of the membrane, impedes crystallization.

In 1999, the first X-ray structures became available for a number of fumarate reductase (FRD) enzymes with dicarboxylate sites homologous to that of Complex II. The FDR's of *E. coli*[7] and of *Wollinella succinogenes*[8] have flavoprotein and iron-protein subunits homologous to those of complex II, and like Complex II have membrane-anchor subunit(s) containing quinone reduction sites, which however are somewhat different from those of Complex II. The flavocytochrome c FDR (FCc) of *Shewanella* [9, 10] is a soluble protein with a single subunit and fumarate reductase activity. Despite being coupled to a cytochrome domain instead of an iron-sulfur protein,

the dicarboxylate binding domain of FCc is clearly homologous to that of complex II, and was well ordered in the crystals.

These structures provided the first clear picture of the dicarboxylate binding site. Interestingly, in one of the highest resolution crystals, grown in the presence of fumarate, the active site contained not fumarate but a "malate-like intermediate" which the authors proposed was formed by slow enzymatic hydration of fumarate by FCc[10].

The first structure of a "true" Complex II (i.e. succinate ubiquinol oxidoreductase, E.C.1.3.5.1) was not the mitochondrial complex but that of *E. coli* [11]. The region around the dicarboxylate site, whose ligand was modeled as OAA, was for the most part similar to that in FCc, however the proposed catalytic arginine (R286 in *E. coli*) was poorly ordered and was modeled in an unusual rotamer with the guanidino group turned away from the active site and toward Glu255. In 2005 - 2006, structures became available for the porcine[12] and avian[13, 14] mitochondrial Complex II. The porcine model had no ligand in the dicarboxylate site, and the catalytic arginine was modeled as in the *E. coli* structure. However our chicken structure was striking in that the dicarboxylate site region superimposed very accurately on that of the *Shewanella* FCc, including the malate-like ligand.

The possibility that the same "malate-like intermediate" can be obtained starting from fumarate or OAA (and presumably from succinate or malate), and the implications for the catalytic capabilities of the site, are intriguing. Now we are refining a higher-resolution structure (including data up to 1.7 Å) to obtain an accurate model of the ligand for identification and comparison with that obtained from fumarate in FCc. We also present here the structures of the malonate-bound complex. Attempts to prepare the fumarate-bound complex resulted in the malate-like intermediate or a mixture of that and fumarate. In addition, we are studying the UV-visible spectral changes in the fully oxidized enzyme occurring upon binding of different ligands, including slow changes taking place after binding, to monitor the contents of the site. Preliminary basis spectra from these studies are presented here.

## Materials and methods -

Avian Complex II was purified and crystallized as described[13]. Routinely no attempt was made to remove endogenous OAA, and the crystal structure as well as spectral experiments to be described below show that the dicarboxylate site is occupied. Protein purification and crystal growth were carried out at 4°C where the rate of OAA dissociation is extremely slow, however the crystallization setups were done at room temperature, taking about 10 min per tray.

Within either crystal form, crystals of the same form were quite isomorphous. This permitted new structures could be solved by rigid-body refinement of the best previous structure of that form against the new data, followed by introduction of any new ligand and B-factor and positional refinement interspersed with examination and manual rebuilding. In the case of the type 2 (P2<sub>1</sub>, pseudo-orthorhombic) crystals it was necessary to make a consistent choice of two non-equivalent possibilities for indexing in order for rigid-body refinement to work, as the lattice has higher symmetry than the unit cell contents.

The malonate-loaded crystal was obtained by co-crystallization: 200 µl of 0.42 mM Complex II (in 20 mM TrisHCl pH 7.5, 0.5 mM EDTA, and 10 g/L octyl glucoside) was treated with 2 µl of 0.1 M disodium malonate for a final concentration of 1 mM and stoichiometric ratio of 2.4 to 1. Then 15 µl aliquots of this were mixed with 15 µl of the precipitant and 1 µl of the additive described[13] to give final concentrations of 0.21 mM protein, 10 g/l (34 mM) octyl glucoside, 50 mM HEPES pH 7.5, 10 mM TrisHCl pH 7.5, 1.3 mM MgCl<sub>2</sub>, 1.6 mM MnCl<sub>2</sub>, 50 g/l PEG 3350, 15 ml/L PEG 400, 25 ml/L isopropanol, 1.5 mM NaN<sub>3</sub>, and 0.25 mM EDTA; and equilibrated against the precipitant by vapor diffusion in the sitting drop format. One of the resulting type 1 crystals was used to collect a dataset to 2.4 Å on beamline 5.0.2 at the Advanced Light Source (ALS), Berkeley CA.

The highest resolution structure containing TEO was obtained in an unsuccessful attempt to ensure complete replacement of the endogenous OAA by fumarate. A two-step exchange was carried out: First the protein was treated with 2 mM malonate at room temperature for about three hours to displace OAA, then it was centrifuged through a

glycerol density gradient, as in the purification procedure[13] except that the gradient contained 5 mM fumarate. The gradient was fractionated, fractions containing Complex II were pooled, and a sample was saved at this stage for spectral analysis. A portion of the remainder was concentrated and exchanged into the usual buffer for crystallization, except that 5 mM fumarate was present. Crystallization was as above. Type 1 crystals formed and some were frozen 30 days after setup. A Diffraction data set was collected and the structure solved to 2.4 Å from one of these. Later type 2 crystals formed, apparently at the expense of the type 1 crystals, in most of the wells. As part of another experiment, some of the wells were treated with short-chain ubiquinone analogs Q1 or Q2 on day 49. It was not noted at the time, but presumably type 2 crystals were already present at this time. Type 2 crystals were frozen at day 54 and 61 after setup, and three of these yielded high resolution (<2.0 Å) datasets. The one selected for refinement and deposition to illustrate the TEO ligand (as NEW1) was from a well treated with Q2, however there is no indication from density at the Q site that Q2 bound there. The dataset was collected at beamline 5.0.2 at the ALS.

Preliminary standard reference spectra for the unliganded enzyme and for the spectral changes induced by OAA, fumarate, malonate, and 3-nitropropionic acid were obtained as described in Results. Experimental spectra were fit to a linear combination of basis spectra as described [15], using wavelength points at 0.1 or 0.2 nm intervals in the range 400 - 700 nm. In order to allow for baseline drift, two additional spectra consisting of a constant offset and a slanted line were always included in the fitting basis set.

## Results

### 1. A high-resolution structure of the “malate-like intermediate”.

As reported [14] crystals of avian complex II from preparations either containing the endogenous inhibitor or treated with OAA both appear to have a ligand in the dicarboxylate site identical to the "malate-like intermediate" seen in high-resolution structures of the *Shewanella frigidimarina* Fcc FRD [10]. For purposes of discussion in

this paper, we refer to this "malate-like ligand" as TEO, the 3-letter ligand ID assigned to it in the PDB. The identity of that ligand is the main subject of ongoing studies of which this paper is a preliminary report. Now we have collected data from two crystals diffracting to 1.7 Å, although due to constraints of detector geometry the data is complete to only 1.9 Å. One of these datasets has now been refined to a Free R-factor of 20.9 (Table 1), giving a very clear picture of the ligand in the dicarboxylate site. During the last stages of refinement we reduced the topology restraints for the ligand, maintaining the bond definitions to avoid nonbonded repulsion but setting the energy terms for bond lengths, angles, dihedrals, and impropers to zero, thus effectively refining free atoms against the X-ray data. Non-crystallographic positional restraints were enforced for the atoms of the ligand, as there was no indication of or reason to expect asymmetry between the buried ligands in the two monomers of the non-physiological dimer present in the asymmetric unit.

Figure 1 shows, in the top panel, a stereo view of the structure around the dicarboxylate site, with the 2Fo-Fc electron density map superimposed. As described at lower resolution for structure 1YQ3 [14], the ligand lies flat on the plane of the FAD isoalloxazine ring, held in place by numerous H-bonds, but with the C1 carboxylate which extends beyond the edge of the ring twisted about 60° out of the plane of the rest of the molecule.

The lower panel compares the dicarboxylate site of our structure with that of that of *Shewanella* FCc (PDB ID 1QJD). The structures are superimposed in such a way as to minimize the RMS deviation between the protein backbone in highly conserved regions surrounding the active site. Although the ligands themselves were not used in the structural alignment, their superposition is nearly perfect, with RMS deviations of 0.25 Å for the 9 atoms and maximum displacement of any atom 0.37 Å.

Since the origin of the ligand in NEW1 is somewhat uncertain, and as described below is likely to be fumarate as in the *Shewanella* structure (because we were attempting to prepare crystals loaded with fumarate, see materials and methods), we also compared it with our previous structure 2fbw in which the endogenous inhibitor, presumed to be OAA, is present. After superposing the backbones of the flavoprotein subunits, the 18 atoms of the ligands in both monomers superimposed with RMSD 0.21 Å. The

conclusion that the same ligand is present in all three structures seems inescapable. that is, the tightly bound inhibitor in the OAA-inhibited enzyme is the same as the "malate-like intermediate" TEO visualized in fumarate-treated *Shewanella* FCc FRD.

Bond lengths, angles and dihedral angles for the TEO ligand in each monomer of the new structure and in the *Shewanella* structure are given in Table 2, which not only confirms the similarity to the FCc structure but may be useful in assigning double vs single bonds and sp<sup>2</sup> vs sp<sup>3</sup> centers, although an unambiguous determination of such details from the x-ray data would require even higher resolution. Care must be taken in not to over interpret the data. The long C1-C2 bond and the non-flat dihedral about this bond suggest it is a pure single bond not involved in a conjugated double bond system. The shorter bonds between C2-C3 and C3-C4 suggest these bond may be double or conjugated. The long C2-O2 bond is more compatible with a single bond, i.e. -OH rather than =O. Further interpretation will be held for the discussion.

## **2. Binding of malonate in the dicarboxylate site.**

In contrast to the attempt to prepare the fumarate-loaded complex, crystallization in the presence of malonate gave the expected result. Figure 2 shows the dicarboxylate site of a crystal prepared from malonate-treated Complex II. The resolution is not as high as the structure described above, but the density is clearly consistent with a shorter dicarboxylate the size of malonate. One carboxylate of malonate is in essentially the same place as the C1 carboxylate of TEO, bonded to Thr265 and the backbone N of Glu266. the difference in length of the ligands thus puts the other carboxylate somewhat short of the position of the C4 carboxylate of TEO. The difference is accommodated partly by movement of the guanidino group of Arg408 towards the ligand and partly by longer H-bonds to that residue.

## **3. Spectroscopic analysis of the state of the dicarboxylate site.**

It has long been known that binding of OAA and other inhibitors is accompanied by subtle but distinct changes in the spectrum of the oxidized enzyme. As an aid in characterizing different batches of the enzyme and in studying binding at the dicarboxylate site, we are obtaining spectra of the changes induced by ligand binding.

The OAA effect is taken as the negative of the slow change occurring when OAA is removed from the enzyme by treatment with transaminase and 10 mM L-glutamate as described in the legend to Figure 4. Raw difference spectra from such an experiment are shown in Figure 4a, in which isobestic points suggest a single change is taking place. The dissociation was fit well by a single exponential (Figure 4b), allowing extrapolation to infinite time to obtain the spectrum of the unliganded enzyme. The reaction was repeated at different temperatures and the Arrhenius plot (Figure 4 inset) indicates an activation energy of 25.4 kcal/mol, similar to the value obtained by for activation of SDH by anions and pH, but lower than the value (33 kcal/mol) found for activation by substrates or ubiquinol. In one case aspartate and  $\alpha$ -ketoglutarate were added to regenerate OAA after stripping was nearly complete, and the immediate spectral change induced by rebinding of OAA was indistinguishable from the slow change observed during dissociation (but with greater extent). The same spectral change was also observed (not shown) on treatment with malate; in fact this treatment yielded the largest OAA-effect spectrum, which we assume corresponds to 100% occupancy with the tightly bound ligand. This is consistent with the observation [5] that addition of malate to activated enzyme leads to inactivation and tightly-bound OAA as assayed by perchlorate extraction. Note that although we refer to this spectral change as the "OAA effect", the precise nature of the bound ligand in the OAA- inhibited enzyme is still under question.

Spectral effects of malonate, fumarate, and 3-nitropropionic acid were obtained by adding the ligands at appropriate concentrations after nearly all the OAA was removed by transamination. Our current set of standard spectra for the ligand-induced changes is shown in Figure 5. The effects of fumarate, malonate, and 3-nitropropionate are similar but distinguishable, and consistent with a perturbation of the spectrum of oxidized flavin in that they do not extend to longer wavelength than about 550 nm. The similarity of the nitropropionate effect with those of fumarate and malonate suggests that on this time scale (10-20 minutes) simple non-covalent binding takes place, and the covalent modification reported [14] requires longer incubation.

The effect of OAA binding is quite different, and involves significant changes over the wavelength range up to 700 nm, where oxidized flavin has little or no absorbance. This long-wavelength absorbance change suggests a long range structural perturbation

that affects the iron-sulfur clusters, or a redox effect involving iron-sulfur clusters or perhaps flavin semiquinone.

**Ligand-status of the protein sample from which the crystal yielding the high-resolution TEO structure was prepared.** As described above, attempts to replace OAA by fumarate for crystallization led to a structure containing the malate-like intermediate TEO in the dicarboxylate site.

A portion of the pooled fractions from the fumarate-containing density gradient was taken and the spectrum recorded with no further treatments to evaluate the effectiveness of fumarate exchange. As Figure 6 shows, this spectrum could be fit well using the spectrum of unliganded complex II, the OAA effect, and the fumarate effect. Of the latter, the OAA effect is much more prominent, being present at a higher level relative to the complex II spectrum than in any of our untreated preparations to date. Only a preparation treated with malate showed a higher level of the OAA effect, presumably due to the highly spontaneous if kinetically limited oxidation of malate to OAA by complex II and any endogenous quinone. The molar extinction scale of the OAA effect has been derived assuming that the malate-treated preparation has 100% OAA occupancy, and applying this scale to the experiment of Figure 6 indicates that 78% of complex II has OAA bound. Similarly the amount of fumarate effect corresponds to 22% of complex II having fumarate bound. The fact that these add up to 100% must be largely fortuitous, given the crude state of our normalization, however it would in fact be expected that nearly all sites would be occupied as fumarate concentration (5 mM) is well above the  $K_d$

#### **Apparent conversion of fumarate to OAA by the Complex II preparation.**

To test more directly for conversion of fumarate to OAA, a sample of Complex II from a preparation that happened to be relatively depleted in OAA was treated with fumarate and spectra were taken at intervals. The spectra were fit using unliganded complex II and the fumarate and OAA effects from Figure 5. The amount of each required is plotted in Figure 7a as a function of time the spectrum was taken. There is a sharp increase in the fumarate effect immediately after addition of fumarate, as expected. However the fumarate effect soon levels off and starts to decrease. The OAA effect was

decreasing slightly during this time, perhaps due to re-equilibration after dilution of the enzyme and competition from the fumarate, but starts to increase again after about 20 minutes. The subsequent gradual increase mirrors the decrease in the fumarate effect.

Difference spectra representative of the fast phase and slow phase are shown in Figure 7b, and their composition from the basis spectra in Figures 7c and 7d. Clearly the fast phase consists mainly of fumarate binding, and the slow phase consists of replacement of bound fumarate by bound OAA. This appears consistent with the idea that fumarate is being converted to OAA.

## **Discussion**

The experiment of Figure 7, as well as the observation of TEO in NEW1 from material treated with fumarate, suggests that long incubation with fumarate can lead to the same inhibited state of the enzyme as OAA or the endogenous inhibitor. This would explain the observation that after activation by succinate the enzyme eventually returns to a partially inactivated state, whereas activation by malonate is stable for long periods of time. It was reported [5] that fumarate or low concentrations of succinate result in gradual deactivation of the activated enzyme, which was attributed to formation of OAA as a result of fumarate contamination and the malate dehydrogenase activity of complex II. Clearly it is important for us to determine if our preparation contains fumarate, perhaps by assaying malonate-insensitive fumarate activity coupled to malate dehydrogenase. We have not eliminated the possibility that contaminating fumarate is responsible for the apparent conversion we see, but the mechanism proposed by Taylor et al for formation of the malate-like inhibitor would also be a reasonable explanation.

If we assume the same tightly bound ligand is present in the inhibited enzyme obtained with fumarate or OAA, the next question is, what is it?. Covalently it has the structure of OAA or malate. While we cannot rely too strongly on bond lengths and angles obtained from X-ray diffraction at this resolution, the data of Table 2 can suggest the geometry of the model. The out-of-plane c1 carboxylate and long c1-c2 bond would be consistent with malate or with a distorted OAA in which the conjugation between the keto or enol double bond and the C1 carboxylate has been broken by the torsion, The short C2-C3 and C3-C4 bonds would be consistent with enol-OAA with the central

double bond conjugated with the C4 carboxylate. It would be also consistent with the tautomer of malate depicted in Fig 4b of Taylor et al. [10].

The main distinction between malate and OAA is their reduction level. Formation of OAA from fumarate via malate, or removal of malate after conversion to OAA, should involve an oxidation step which would leave two electrons on the enzyme, presumably residing in the high potential iron-sulfur centers 1 and 3. While the broad bleaching extending to 700 nm associated with the stripping reaction (Figure 5) is suggestive of reduction of iron-sulfur centers, the reverse spectrum is obtained on adding OAA to (presumably oxidized) enzyme, in which case it could not be an effect on redox state of the iron-sulfur proteins.

If the ligand were actually malate the twisted conformation would not be particularly unstable, as there are no double bonds beside the carboxylates. However given the redox midpoint potential of the malate/OAA couple ( $\sim -166$  mv in solution) and the Flavin, and the MDH activity of the complex, it would seem that malate could not exist in the binding site with oxidized flavin for long. This conclusion would not hold if malate were to bind much more tightly than OAA, lowering the midpoint potential of the bound couple relative to free.

However if the tightly bound form is malate, it must be oxidized before release as OAA, so activation by transaminase would be expected to result in two-equivalent reduction of the enzyme. While the broad bleaching observed during activation by treatment with transaminase is reminiscent of Fe-S protein reduction, this spectrum is just the opposite of what is obtained when OAA binds to the (presumably fully oxidized) stripped complex, in which case redox changes of the Fe-S proteins could not account for the broad increase in absorbance. Further experiments with electron acceptors (PMS/DCIP) and using transaminase to strip the enzyme after loading from malate or OAA may help resolve the issue.

**Acknowledgements-** This work was supported by NIH R01 grants GM62563) and DK44842 and was carried out at Lawrence Berkeley National Lab, which is operated by the Department of Energy, contract DE-AC03-76SF00098 to the University of California. Diffraction data were collected at the Advanced Light Source (ALS) at LBNL and at the Stanford Synchrotron Radiation Laboratory, which is operated by the Department of

Energy, Office of Basic Energy Sciences. We thank staff at the various beamlines for help and advice in data collection.

**Footnotes.**

1. Abbreviations used are: OAA, oxaloacetate. MDH, malate dehydrogenase. FCc, flavo-cytochrome c. TEO, the "malate-like intermediate" found in 1QJD. Complex II, succinate ubiquinone oxidoreductase; E.C. 1.3.5.1. Q1 and Q2, ubiquinol with only 1 or two isoprenoid units in the side-chain. The coordinates for the two structures described here have been deposited with the PDB as NEW1 (TEO-containing structure) and NEW2 (malonate-containing structure).

## References

- [1]E.B. Kearney, Studies on succinic dehydrogenase. IV. Activation of the beef heart enzyme, *J Biol Chem* 229 (1957) 363-75.
- [2]E.B. Kearney, B.A. Ackrell and M. Mayr, Tightly bound oxalacetate and the activation of succinate dehydrogenase, *Biochem Biophys Res Commun* 49 (1972) 1115-21.
- [3]A.B. Kotlyar and A.D. Vinogradov, Interaction of the membrane-bound succinate dehydrogenase with substrate and competitive inhibitors, *Biochim Biophys Acta* 784 (1984) 24-34.
- [4]D.V. Dervartanian and C. Veeger, Studies on succinate dehydrogenase. II. On the nature of the reaction of competitive inhibitors and substrates with succinate dehydrogenase, *Biochim Biophys Acta* 105 (1965) 424-36.
- [5]B.A. Ackrell, E.B. Kearney and M. Mayr, Role of oxalacetate in the regulation of mammalian succinate dehydrogenase, *J Biol Chem* 249 (1974) 2021-7.
- [6]Y.O. Belikova, A.B. Kotlyar and A.D. Vinogradov, Oxidation of malate by the mitochondrial succinate-ubiquinone reductase, *Biochim Biophys Acta* 936 (1988) 1-9.
- [7]T.M. Iverson, C. Luna-Chavez, G. Cecchini and D.C. Rees, Structure of the *Escherichia coli* fumarate reductase respiratory complex, *Science* 284 (1999) 1961-6.
- [8]C.R. Lancaster, A. Kroger, M. Auer and H. Michel, Structure of fumarate reductase from *Wolinella succinogenes* at 2.2 Å resolution, *Nature* 402 (1999) 377-85.
- [9]D. Leys, A.S. Tsapin, K.H. Nealson, T.E. Meyer, M.A. Cusanovich and J.J. Van Beeumen, Structure and mechanism of the flavocytochrome c fumarate reductase of *Shewanella putrefaciens* MR-1, *Nat Struct Biol* 6 (1999) 1113-7.
- [10]P. Taylor, S.L. Pealing, G.A. Reid, S.K. Chapman and M.D. Walkinshaw, Structural and mechanistic mapping of a unique fumarate reductase, *Nat Struct Biol* 6 (1999) 1108-12.
- [11]V. Yankovskaya, R. Horsefield, S. Tornroth, C. Luna-Chavez, H. Miyoshi, C. Leger, B. Byrne, G. Cecchini and S. Iwata, Architecture of succinate dehydrogenase and reactive oxygen species generation, *Science* 299 (2003) 700-4.
- [12]F. Sun, X. Huo, Y. Zhai, A. Wang, J. Xu, D. Su, M. Bartlam and Z. Rao, Crystal Structure of Mitochondrial Respiratory Membrane Protein Complex II, *Cell* 121 (2005) 1043-57.
- [13]L.S. Huang, T.M. Borders, J.T. Shen, C.J. Wang and E.A. Berry, Crystallization of mitochondrial respiratory complex II from chicken heart: a membrane-protein complex diffracting to 2.0 Å, *Acta Crystallogr D Biol Crystallogr* 61 (2005) 380-7.
- [14]L.-S. Huang, G. Sun, D. Cobessi, A.C. Wang, J.T. Shen, E.Y. Tung, V.E. Anderson and E.A. Berry, 3-nitropropionic acid is a suicide inhibitor of mitochondrial respiration that, upon oxidation by complex II, forms a covalent adduct with a catalytic-base arginine in the active site of the enzyme, *J. Biol. Chem.* 281 (2006) 5965-5972.

- [15]J. Sternberg, H. Stillo and R. Schwendeman, Spectrophotometric Analysis of Multicomponent Systems Using the Least Squares Method in Matrix Form, *Analytical Chemistry* 32 (1960) 84-90.
- [16]E.A. Berry and B.L. Trumpower, Simultaneous determination of hemes a, b, and c from pyridine hemochrome spectra, *Anal Biochem* 161 (1987) 1-15.

**Table 1. Data processing and refinement statistics for structure new1, with TEO at the active site, and new2, with malonate.**

PDB ID code	<b>NEW1-2803*</b>	<b>NEW2-908*</b>
Ligand modeled	TEO <sup>1</sup>	malonate
Space Group	P2 <sub>1</sub>	P2 <sub>1</sub> 2 <sub>1</sub> 2 <sub>1</sub>
Cell parameters	120.1 199.4 68.0 90 90.00 90	70.5 84.0 291.6 90 90 90
Resolution range	45 - 1.74 Å	50.68 - 2.4 Å
(last shell)	(1.70-1.74)	(2.40 - 2.46)
Completeness	87.0% (38.8%)	85.4% (43.8%)
# Reflections	304101 (8542)	58846 (1881)
Cryst. R Value	0.181 (0.348)	0.230 (0.38)
Free R Value	0.209 (0.354)	0.286 (0.44)
B Values		
From Wilson Plot	23.8 Å <sup>2</sup>	51.8 Å <sup>2</sup>
Mean atomic B Value	32.4 Å <sup>2</sup>	61.7 Å <sup>2</sup>
RMS Deviations from Ideality:		
Bond Lengths	0.024 Å	0.012 Å
Bond Angles	2.0°	1.6°
Dihedral Angles	22.7°	22.2°
Improper Angles	1.30°	0.92°

\*If the paper is accepted the correct pdb ID codes will be inserted in the final manuscript.

1. TEO: the malate-like intermediate described in the *Shewanella* FCc active site[10].

Table 2: Approximate bonds and angles for TEO from the structures. For each parameter, three values are given: one from *Shewanella* structure 1QJD, and one from each monomer of Complex II structure NEW1.

Bond Lengths:			1QJD	new1a	new1b	comment:
C1	O1A		1.178	1.259	1.263	
C1	O1B		1.216	1.293	1.278	
C2	O2		1.318	1.438	1.360	C-OH bond, longer than C=O
C2	C1		1.601	1.630	1.699	single bond, no resonance
C3	C2		1.376	1.332	1.376	double bond? ene-ol?
C4	C3		1.369	1.504	1.492	resonance?
C4	O4A		1.323	1.258	1.262	
C4	O4B		1.487	1.282	1.301	

Bond Angles				1QJD	new1a	new1b	comment:
O1A	C1	O1B		133.01	126.78	128.97	
C2	C1	O1B		108.97	109.55	107.58	
C2	C1	O1A		116.51	123.55	123.45	
C1	C2	O2		114.66	104.20	102.69	
C3	C2	O2		131.65	142.16	148.39	???
C1	C2	C3		109.09	113.47	108.86	
C2	C3	C4		119.47	105.55	102.17	
O4B	C4	C3		120.59	125.60	127.42	
O4A	C4	C3		130.80	106.21	105.38	
O4A	C4	O4B		107.31	121.24	120.96	

Dihedral angles:				1QJD	new1a	new1b	comment:
O4B	C4	C3	C2	1.40	-179.42	177.59	C3-C4 dihedral
C3	C2	C1	O1A	89.52	57.93	61.59	C1-C2 dihedral, measured to c3
O2	C2	C1	O1B	56.23	65.31	63.13	C1-C2 dihedral, measured to O2
Improper dihedral angles:				1QJD	new1a	new1b	comment:
C4	O4A	O4B	C3	6.238	19.079	17.838	C4 Carbox dished?
C2	C3	C1	O2	11.648	-2.271	-1.232	C2 Center flat?
C1	C2	O1A	O1B	-7.287	2.371	-0.295	C1 Carbox flat.

## Figure Legends

**Figure 1. Overall view of Complex II, detail of Fe<sub>3</sub>S<sub>4</sub> cluster.** The dicarboxylate site, represented by the green stick figure of the "malate-like ligand" found in the inhibited-inhibited complex, is in the Flavoprotein subunit (Yellow and magenta). A series of three iron-sulfur clusters bridge the gap between Flavin at the dicarboxylate site (blue) and the quinone binding site (yellow ubiquinone headgroup). **(B)** The Fe<sub>3</sub>S<sub>4</sub> cluster in the high-resolution TEO containing structure NEW1. The 2Fo-Fc map is contoured at 15  $\sigma$  (magenta) to show the iron atoms, and at 6  $\sigma$  (cyan) to show the sulfurs as well. The irons and sulfurs, separate by about 2.2 Å, are well resolved in this structure.

**Figure 2. Stereo view of the malate-like ligand** in a 1.8 Å structure currently being refined. Note how the C1 carboxylate is twisted out of the plane of the rest of the molecule which lies flat against the plane of the FAD isoalloxazine ring. **(A)**. 2Fo-Fc map contoured at 1.7  $\sigma$ .

**Figure 3. Stereo view of malonate in the dicarboxylate site** of complex II co-crystallized with the inhibitor. . 2Fo-Fc map

**Figure 4. (A) The spectral effect of OAA binding** was determined by following the dissociation of OAA from Complex II when the free concentration of OAA is held well below the dissociation constant using transaminase and glutamate [3]. One ml of 20 mM KMOPS 7.2, 100 mM NaCl, 0.5 mM EDTA, and 0.1 g/l dodecyl maltoside was supplemented with 10  $\mu$ l 0.1 M Na-glutamate and a baseline was recorded. Then 75  $\mu$ l of complex was added and scanned several times to get the spectrum of the as-purified material. Then 1  $\mu$ l of glutamate/oxaloacetate transaminase was added and scans were recorded repeatedly during the stripping process, which was followed for five hours. The average of the spectra of Complex II before adding transaminase was subtracted from all, and spectra before and at (times) are plotted. Then (not shown) dithionite was added to obtain the fully reduced spectrum from which the enzyme concentration was determined using the approximate extinction coefficient of 16.8 mM<sup>-1</sup> at 560-542 for the reduced protein [13]. **(B). Time course of dissociation of OAA.** Continuing the experiment of Figure 4a, A spectrum representative of the OAA-induced change was obtained from the spectra of figure 3 and the spectra were fit to a linear combination of that and the starting Complex II spectrum. The resulting amplitude of the OAA effect was plotted against time and fit with a single exponential. The t-infinity value obtained from the fit was taken as the amount of the OAA-effect spectrum to subtract from the initial as-purified spectrum to obtain the spectrum of the fully-stripped enzyme, which was scaled to 1  $\mu$ M based on the concentration determined from the dithionite-reduced spectrum above. The spectrum of the OAA effect was scaled so that the most OAA-laden preparation for which we had spectra gave a ratio of one OAA per Complex II. The spectra were then re-fit using the same OAA effect spectrum and the stripped Complex II spectrum, to obtain the data shown, in which the OAA effect decays toward zero.

**Figure 5. Difference spectra representing the effects of various ligands** on the spectrum of fully oxidized Complex II. Preliminary standard spectra for the spectral

effects of OAA, malonate, fumarate, and 3-nitropropionic acid were determined as described in the text. The magnitude is on an arbitrary scale.

**Figure 6. Spectrum of Complex II after exchange into fumarate for crystallization.**

The blue trace is an experimental spectrum of the Complex II preparation from which the crystal leading to the NEW1 structure was grown. It had been treated with malonate at room temperature for 3 hours and sedimented through a gradient containing 5 mM fumarate as described in materials and methods. The green trace is the best fit to the experimental trace using a linear combination of the spectra of Complex II, the fumarate effect, and the OAA effect. The required magnitude of each of these is shown.

**Figure 7. Time course of spectral changes after adding fumarate to Complex II.**

A. Time course: Each time point represents one spectrum. 10 mM fumarate was added after the second spectrum (arrows). Each spectrum was fit to a linear combination of the empty-site complex, the OAA effect, and the fumarate effect. The amount of each spectrum required to reconstitute the experimental spectrum is plotted against time. (B) shows difference spectra, 14 min vs before fumarate and 460 minutes vs 14 min. (C) and (D) show the fit to these two spectra and the amount of the OAA and fumarate spectral effects required. The slow phase consists mainly of disappearance of the fumarate effect and appearance of the OAA effect.

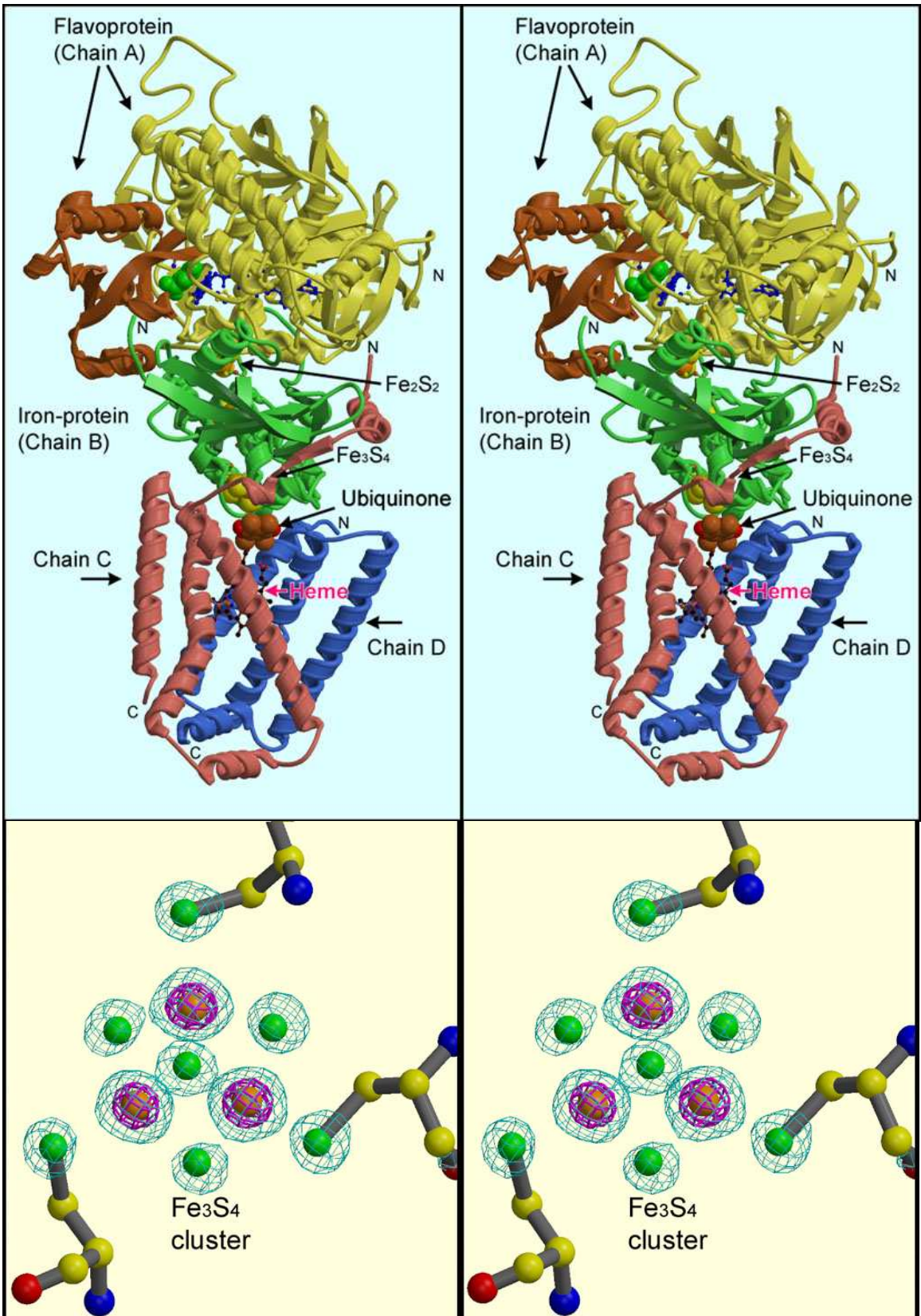


Figure 1.

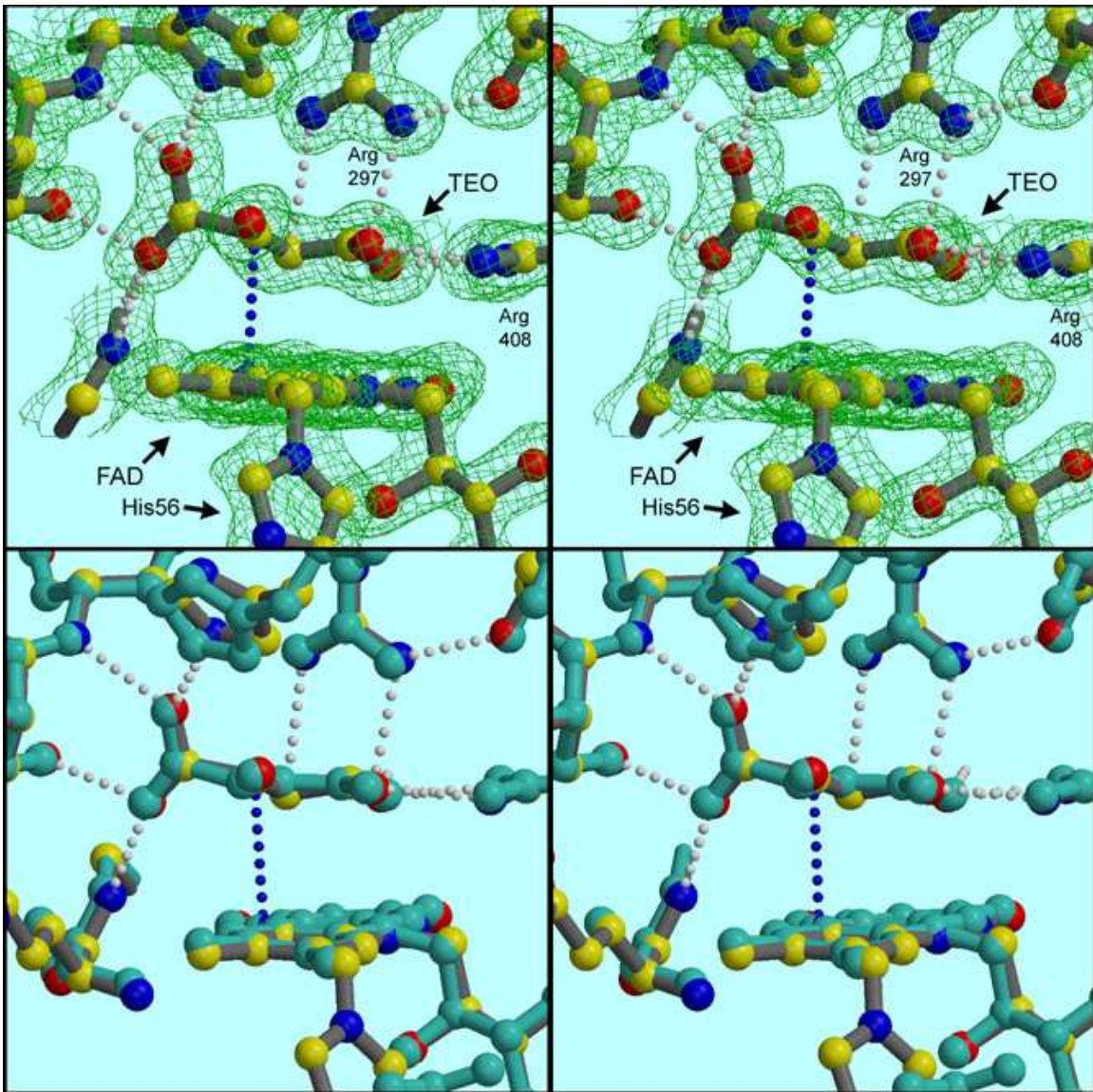
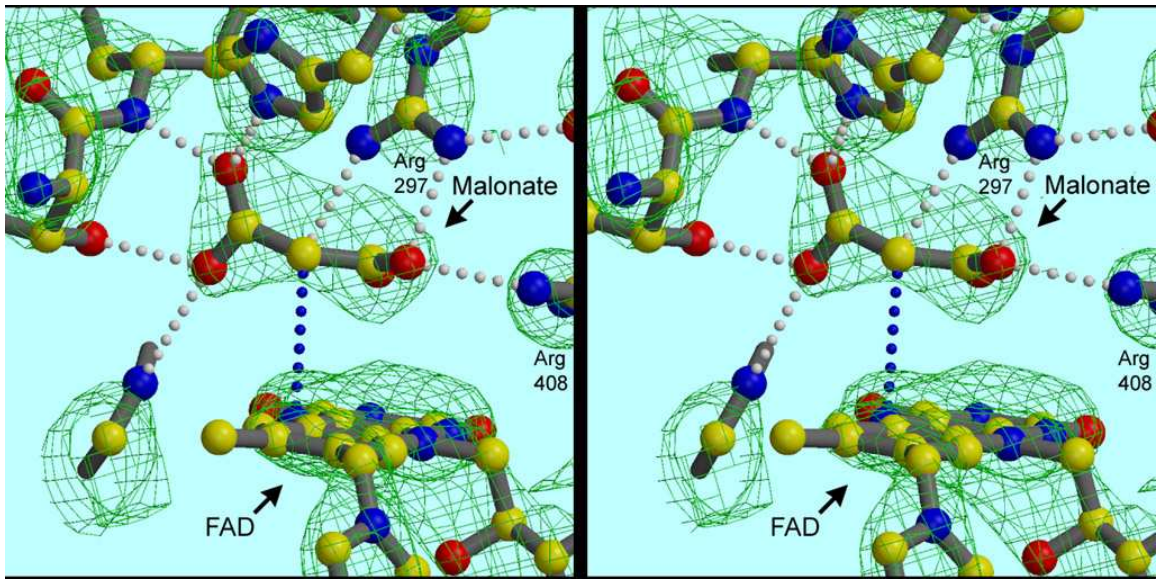


Figure 2.



**Figure 3.**

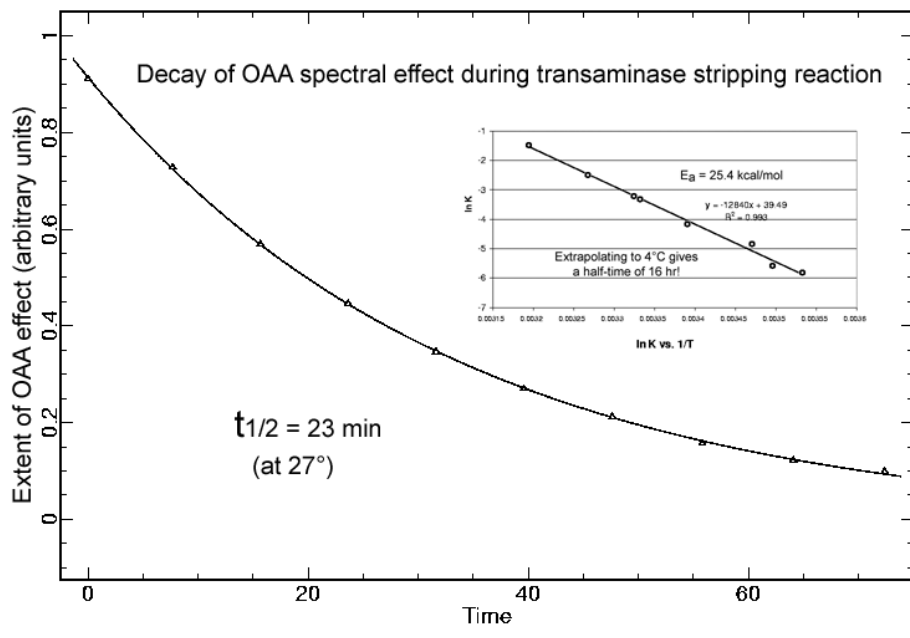
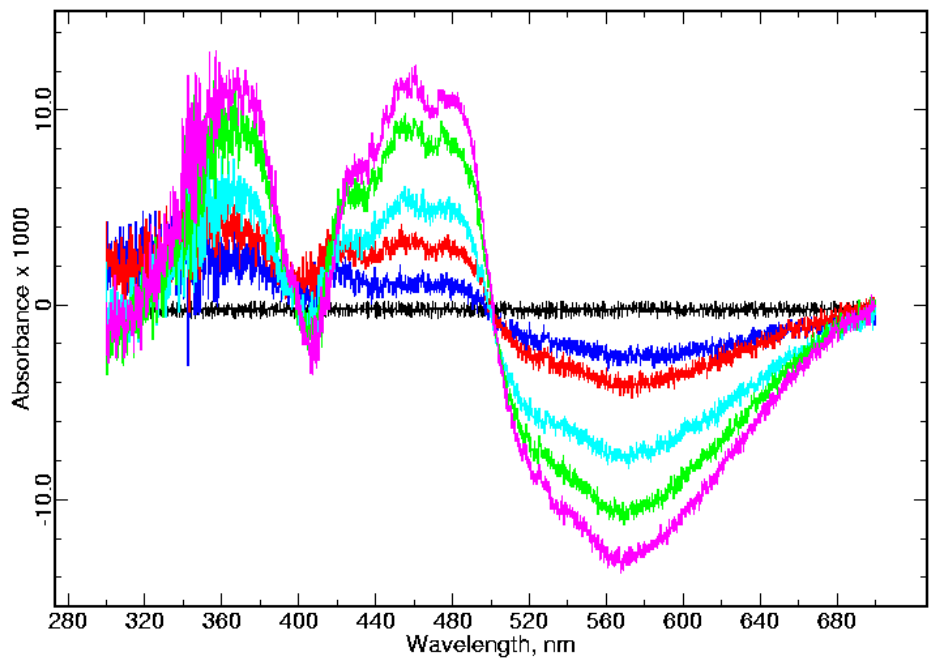
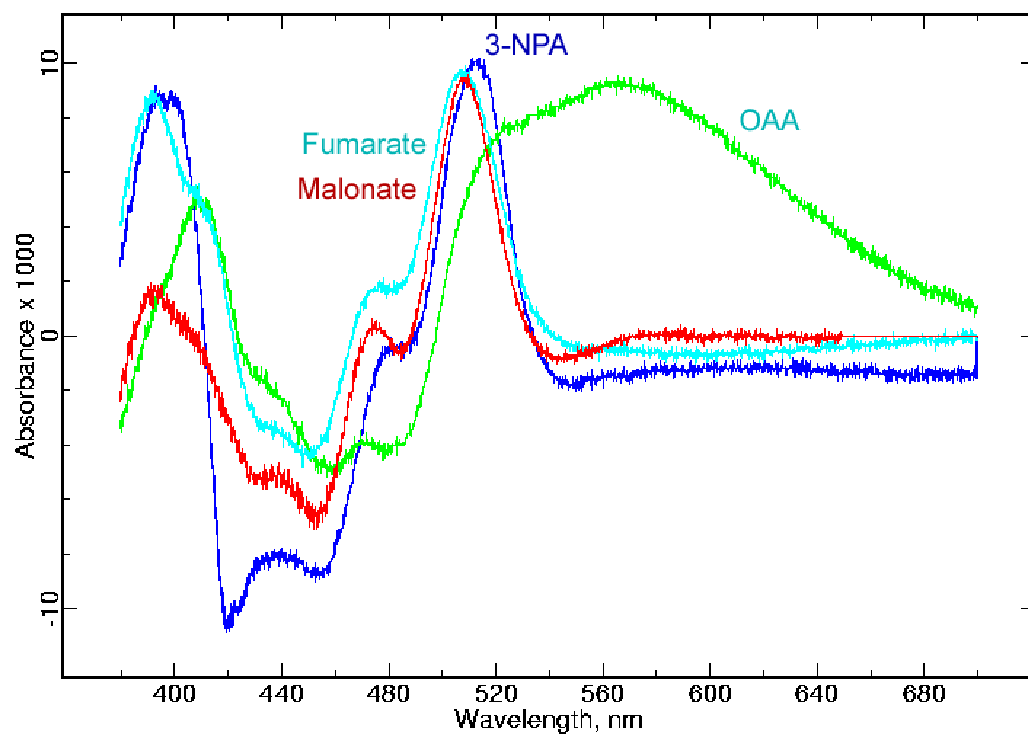


Figure 4



**Figure 5**

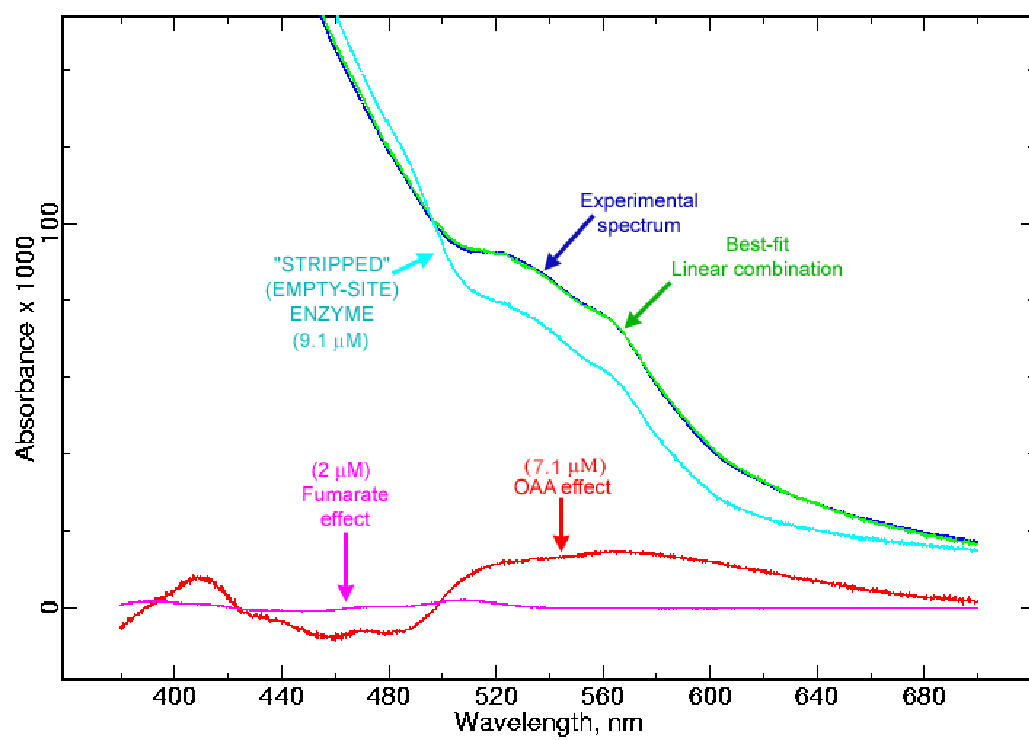


Figure 6.

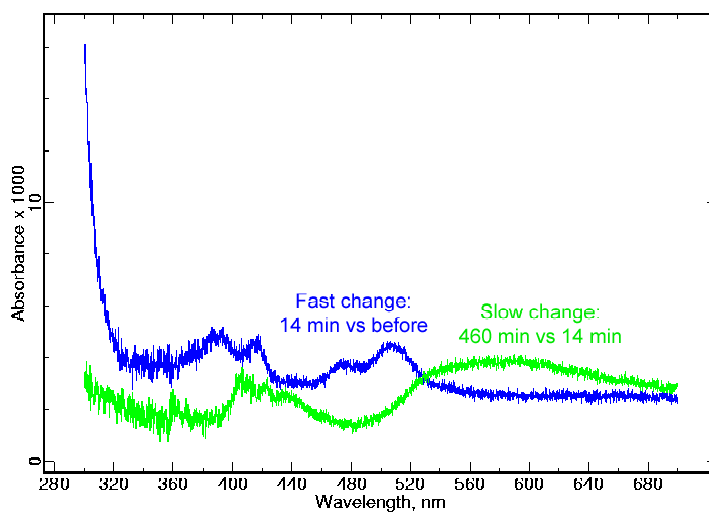
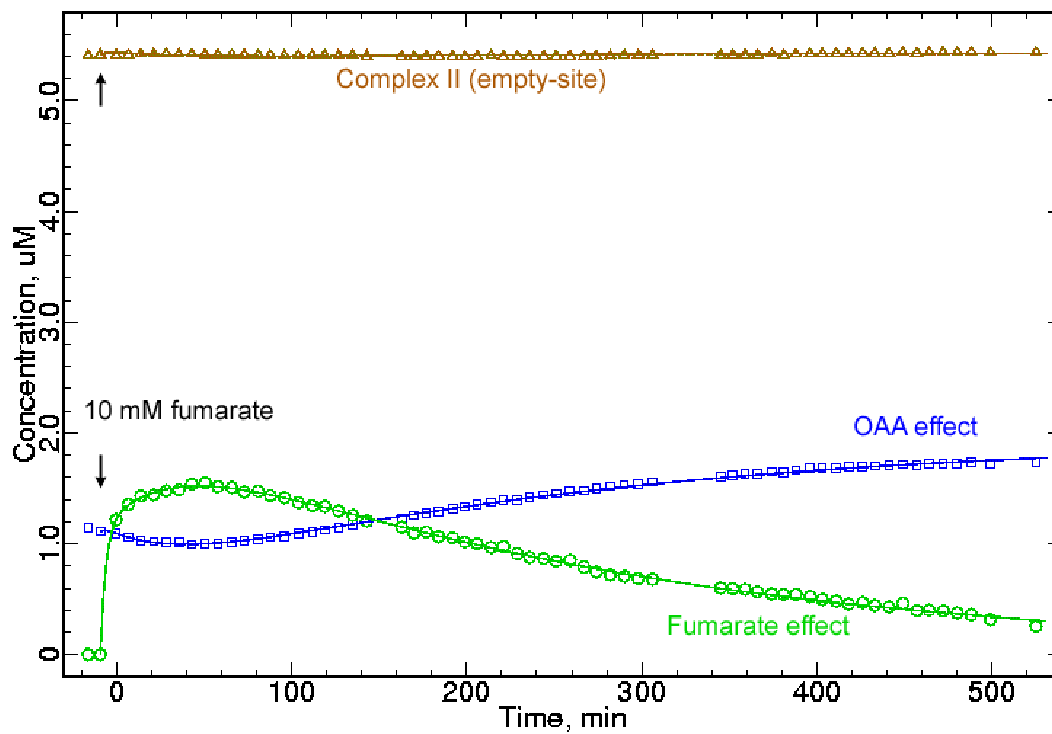


Figure 7 A, B

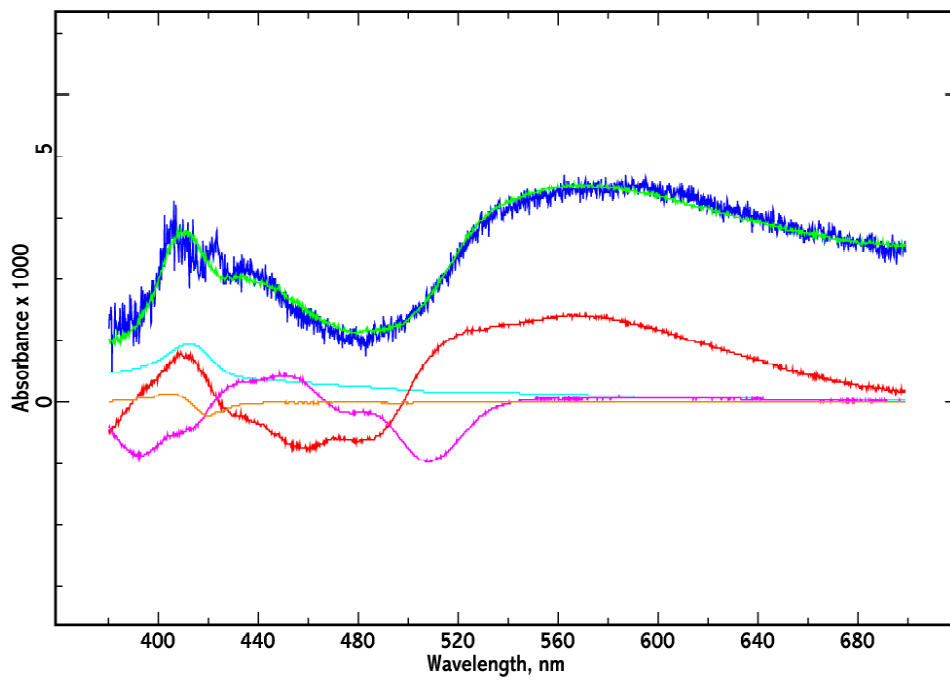
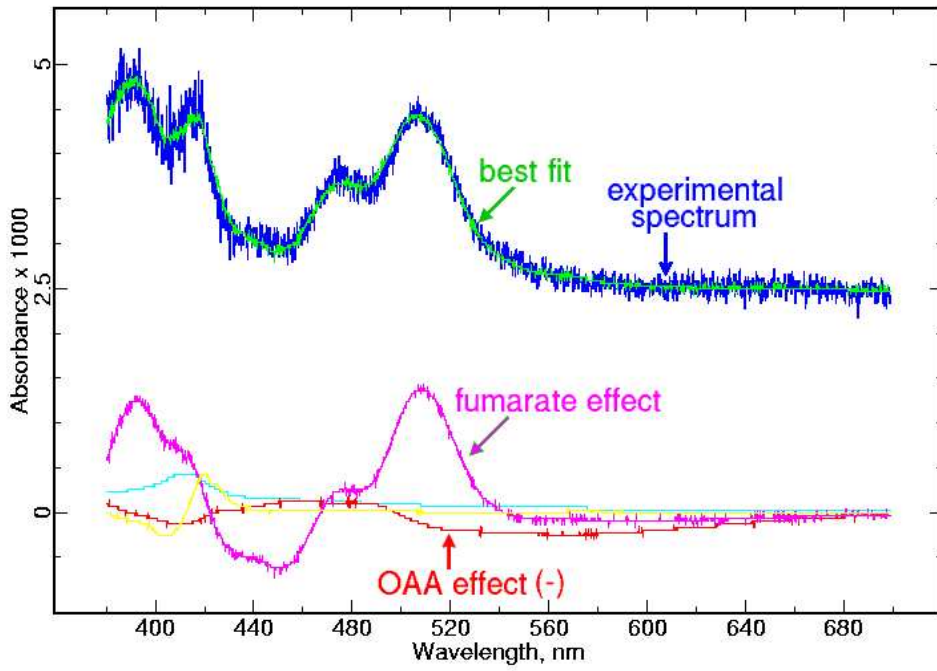


Figure 7 C, D